Title	Growth and magnetic properties of MnAs/InAs hybrid structure on GaAs(111)B
Author(s)	Islam, Md Earul; Akabori, Masashi
Citation	Journal of Crystal Growth, 463: 86-89
Issue Date	2017-02-08
Type	Journal Article
Text version	author
URL	http://hdl.handle.net/10119/15731
Rights	Copyright (C) 2017, Elsevier. Licensed under the Creative Commons Attribution-NonCommercial-NoDerivatives 4.0 International license (CC BY-NC-ND 4.0). [http://creativecommons.org/licenses/by-nc-nd/4.0/] NOTICE: This is the author's version of a work accepted for publication by Elsevier. Md Earul Islam, Masashi Akabori, Journal of Crystal Growth, 463, 2017, 86-89, http://dx.doi.org/10.1016/j.jcrysgro.2017.02.009
Description	

Growth and magnetic properties of MnAs/InAs hybrid structure on GaAs(111)B

*Md. Earul Islam, Masashi Akabori

Center for Nano Materials and Technology (CNMT), Japan Advanced Institute of

Science and Technology (JAIST), 1-1 Asahidai, Nomi, Ishikawa 923-1292, JAPAN

E-mail: s1540002@jaist.ac.jp; akabori@jaist.ac.jp

*Corresponding author, e-mail: s1540002@jaist.ac.jp ; Tel: +81-761-51-1920

Abstract

We carried out molecular beam epitaxial (MBE) growth of MnAs/InAs hybrid structure on GaAs(111)B for spin field effect transistor (spin-FET) applications. We observed good alignment of hexagonal MnAs and cubic InAs epitaxial layers with GaAs(111)B by X-ray diffraction (XRD) measurement. We observed smooth surface morphology of MnAs/InAs by atomic force microscopy (AFM), and also observed maze-like magnetic structure by magnetic force microscopy (MFM). We observed easy and hard magnetizations in-plane and out-of-plane directions similar to MnAs/GaAs(111)B using superconducting quantum interference device (SQUID) magnetometer. We believe that the MnAs/InAs hybrid structure on GaAs(111)B can be a base structure for spin-FETs.

Keywords

A3. Molecular beam epitaxy (MBE); B2. MnAs, InAs, GaAs(111)B; A1. X-ray diffraction (XRD); A1. Atomic force microscopy (AFM); A1. Magnetic force microscopy (MFM); A1. Superconducting quantum interference device (SQUID) magnetometer

1. Introduction

In semiconductor spintronics, ferromagnetic/semiconductor hybrid structures have already attracted attention because of their potential application for spin field effect transistors (spin-FETs) [1]. For spin-FET application, it is necessary to have ferromagnetic source and drain for spin polarized carrier injection and detection, and semiconductor channel with spin-orbit coupling (SOC) controlled by electric field for spin polarized carrier transport. Hexagonal NiAs-type MnAs is a ferromagnetic metal with Curie temperature over room temperature [2], which can be synthesized with III-As semiconductors in epitaxial growth system [3] without unintentional reaction between transition ferromagnetic metals like Fe and As [4]. There is also a demonstration of lateral spin-valve device application using MnAs on GaAs(001) [5], which supports spin polarized carrier injection and detection. III-As semiconductors are expected to show large SOC when the bandgap becomes narrow, and InAs is a narrow bandgap III-As semiconductor. In addition, InAs has surface/interface electron accumulation layers [6] showing good conductivity without intentional doping. Therefore, MnAs/InAs hybrid structures are possible candidates for the base structures of spin-FET application, however, to our knowledge there is only a few

reports on MnAs growth on thin (less than 10 nm) InAs [7, 8] and no report on MnAs growth on thick InAs layer or substrate.

In this paper, we report on molecular beam epitaxial (MBE) growth of a MnAs/InAs hybrid structure on semi-insulating GaAs(111)B, its X-ray diffraction (XRD) measurement results, and its magnetic properties measured using a magnetic force microscope (MFM) and a superconducting quantum interference device (SQUID) magnetometer. We have chosen (111)B as the growth surface. This is because hexagonal NiAs-type MnAs with c-axis normal to the plane has been observed on GaAs(111)B and InP(111)B [9, 10] and has shown almost isotropic in-plane magnetization [11]. At MnAs/InAs and InAs/GaAs interfaces, generation of misfit dislocations due to lattice mismatch (MnAs/InAs: ~14% and InAs/GaAs: ~7%) is expected. Since in the present case on (111)B the sliding planes with 3 sliding directions of MnAs and InAs are expected to be in-plane, the degradation of physical properties by the dislocations is expected to become weaker by networking the dislocations than that on (001). In fact high quality InAs on not GaAs(111)B but GaAs(111)A has been reported [12] and essentially similar effect is expected on (111)B. Therefore, these are expected to be helpful to in-plane type spintronic device application.

2. Layer growth

We used a semi-insulating GaAs(111)B substrate with 12 mm X 15 mm. The substrate was performed organic and inorganic cleaning, and then it was loaded into a conventional solid source MBE system. After preheating of the substrate up to ~370°C in the vacuum, it was transferred into the growth chamber, and the hybrid structure growth was performed. The substrate always exposed to an As ambient with beam equivalent pressure (BEP) of ~1.5×10^{-5} Torr in the growth chamber. After native oxide removal of the substrate surface at ~600 °C in 15 minutes, the substrate temperature was reduced and stabilized at ~480 °C. Then, thick InAs layer growth was carried out in 1 hour with As/In BEP ratio of ~20 directly on the substrate surface without buffer layer. Afterwards, the substrate temperature was again reduced and stabilized at ~250 °C. Then, MnAs layer growth was carried out in 1 hour with As/Mn BEP ratio of ~234. The nominal thicknesses of InAs and MnAs were ~1.2 μm and ~200 nm, respectively. The substrate temperature was monitored with an infrared pyrometer.

3. Epitaxial relations

We studied the crystal structure and the epitaxial relations among different layers of the hybrid structure by XRD measurements. Figure 1 shows the 2θ scanning result between 20° and 80°. 6 peaks can be clearly seen, and the peak positions from low angle side correspond to InAs(111), GaAs(111), MnAs(0002), InAs(222), GaAs(222), and MnAs(0004) labeled in the figure. The MnAs peaks are almost same as those

directly grown on GaAs(111)B, whose differences are less than 0.01°. We extracted a lattice parameter for hexagonal MnAs of $c \sim 5.71$ Å, and lattice parameters for cubic InAs and GaAs of $a \sim 6.06$ Å and $a \sim 5.65$ Å, respectively. The lattice parameters are consistent with their bulk values [7, 13] which imply that the grown epitaxial layers are strain relaxed and lattice mismatch.
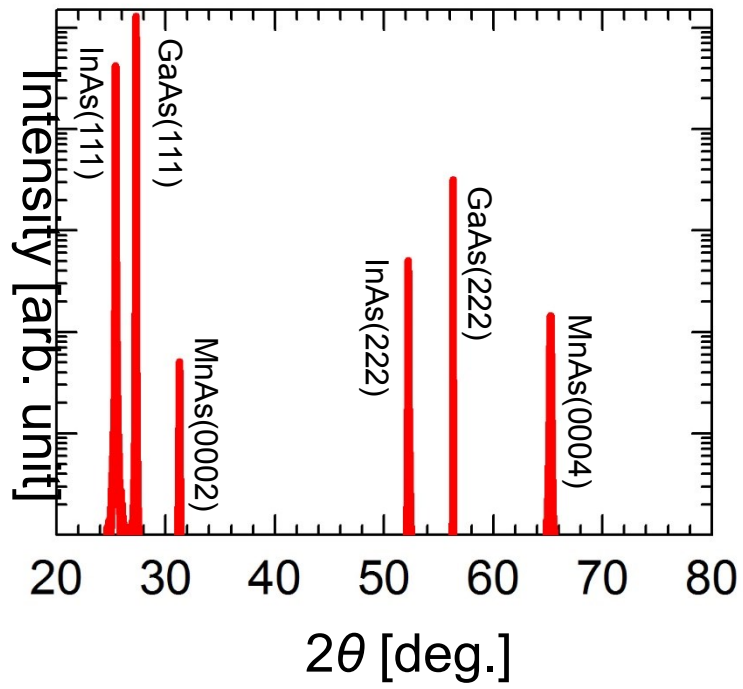
FIG. 1. XRD spectra of MnAs/InAs/GaAs(111)B obtained by 2θ-scanning.

We also carried out ω scanning of InAs(111) and MnAs(0002) to elucidate the deviation of c-axis normal to the planes as shown in Fig. 2. Peak positions are almost zero, i.e. the ω values at the peaks are almost same as the θ values in 2θ scanning. The result indicates almost no tilting of both InAs and MnAs layers to GaAs substrate. Peak broadening of InAs(111) and MnAs(0002) are ~0.12° and ~0.22°, respectively. The result means almost negligible deviation of c-axis of InAs(111) and MnAs(0002) planes. From the broadening we roughly estimated the threading dislocation densities [14] to be 5.5×10^8 and 2.5×10^9 cm^{-2} for InAs and MnAs, respectively. The value for InAs seems relatively smaller than that on (001) assuming same thickness [15]. Hence, from 2θ and ω scanning results, we can conclude good stacking of MnAs(0001)/InAs(111)B on GaAs(111)B.
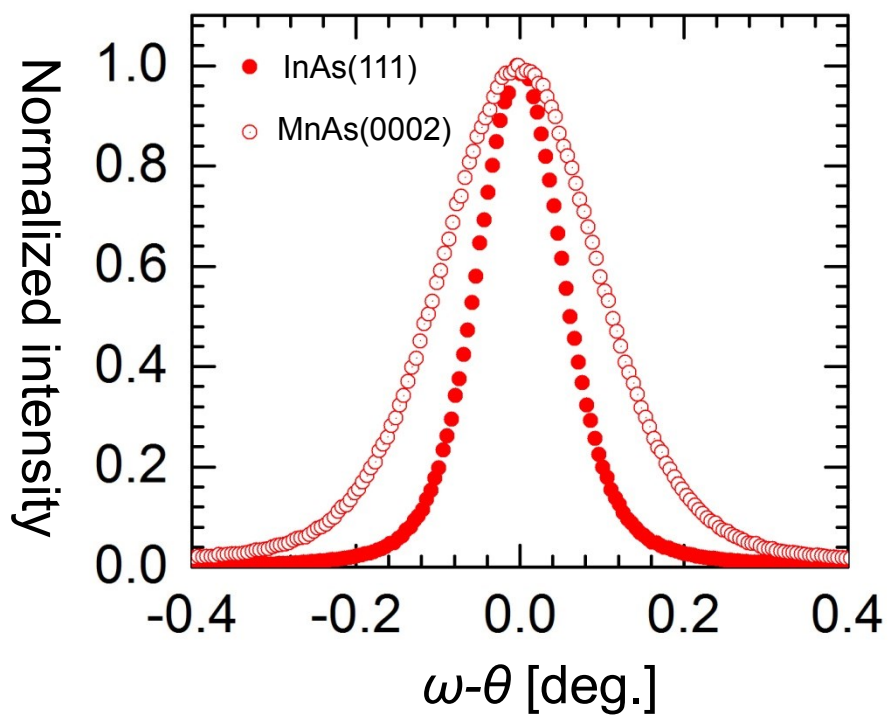
FIG. 2. *ω-θ* scanning curves of InAs(111) and MnAs(0002).

We also performed in-plane φ scanning for MnAs(10-12), InAs(004), and GaAs(004) planes as shown in Fig. 3. The incident X-ray direction at φ = 0° was along [-211] of GaAs(111)B. We confirmed 6-fold rotational symmetry of MnAs, and 3-fold rotational symmetry of InAs and GaAs. The results indicate that MnAs[-2110], InAs[-110], and GaAs[-110] are parallel each other. This result shows good alignment of hexagonal MnAs and cubic InAs epitaxial layers with cubic GaAs substrate.
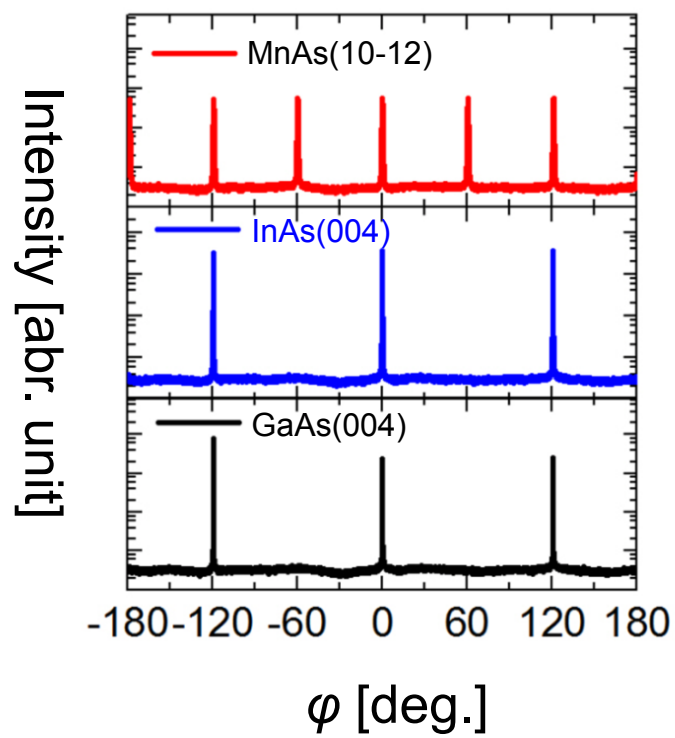
FIG. 3. In-plane φ-scanning for MnAs(10-12), InAs(004), and GaAs(004) planes.

4. Magnetic structure

We also studied surface morphology and magnetic structure of the hybrid structure using atomic force microscopy (AFM) and magnetic force microscopy (MFM) as shown in Fig. 4(a) and 4(b), respectively. We proceeded magnetization of only Co-based cantilever tip before the measurements. The smooth surface can be seen with the root mean square of ~0.8 nm, and also the significant magnetic structure can be seen with maze-like pattern. The surface roughness and the magnetic structure seem almost similar to those of MnAs directly grown on GaAs(111)B, whose roughness is ~0.9 nm. As a result, we conclude that the MnAs layer is ferromagnetic.
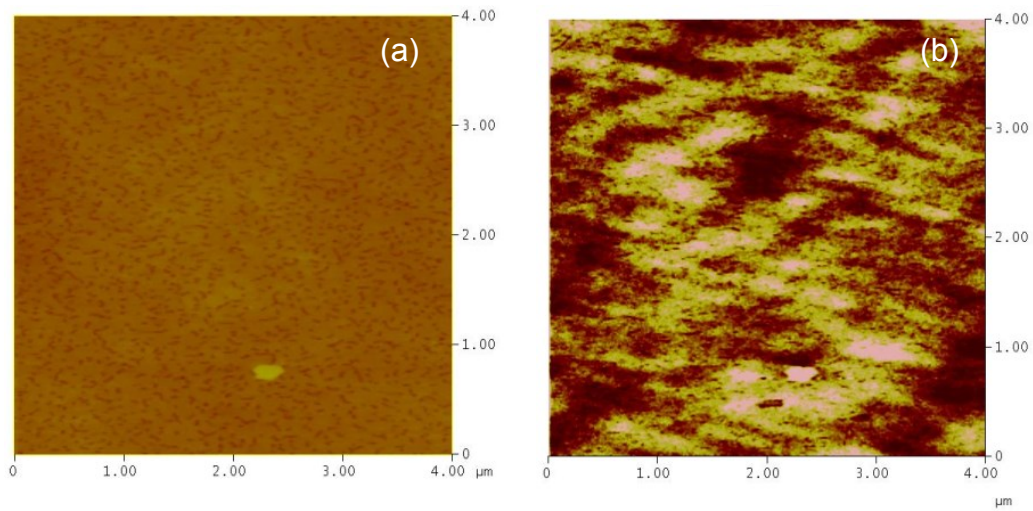
FIG. 4. (a) AFM and (b) MFM images of MnAs/InAs/GaAs(111)B.

5. Magnetization

To confirm detail magnetic properties of the hybrid structure, we performed magnetization (M) measurements using a superconducting quantum interference device (SQUID) magnetometer. We prepared (5x4) mm^2 sample for the measurement. Figure 5(a) and (b) shows the normalized magnetization of the hybrid structure at 300 K as a function of applied magnetic field (H) along to in-plane [-2110] and out-of-plane [0001] of hexagonal MnAs. We found easy magnetization along in-plane direction and hard magnetization along out-of-plane which is similar to MnAs on GaAs(111)B in literature [11], even though we did not measure our MnAs directly grown on GaAs(111)B. The saturation magnetizations (M_S) are ~300 emu/cm^3 and ~200 emu/cm^3 and the coercive fields (H_C) are ~320 Oe and ~600 Oe along in-plane and out-of-plane, respectively which implies strong anisotropy between in-plane and out of plane. Here, we have not subtracted the influence of diamagnetic influence of GaAs and InAs into the magnetization. In the case of in-plane measurement, the magnetic moment of MnAs after the saturation is ~100 times larger than that of diamagnetic GaAs and InAs at 2000 Oe. Therefore, the diamagnetic contribution is almost negligible. However, in the case of out-of-plane measurement, the diamagnetic moment becomes ~15 times larger at 30000 Oe. Therefore, it can give significant contribution into the total magnetic moment and the difference of saturation magnetization between in-plane and out-of-plane measurements. Since

there are also magnetocrystalline anisotropy and demagnetizing field anisotropy, these can give the difference of coercive field between in-plane and out-of-plane measurements.
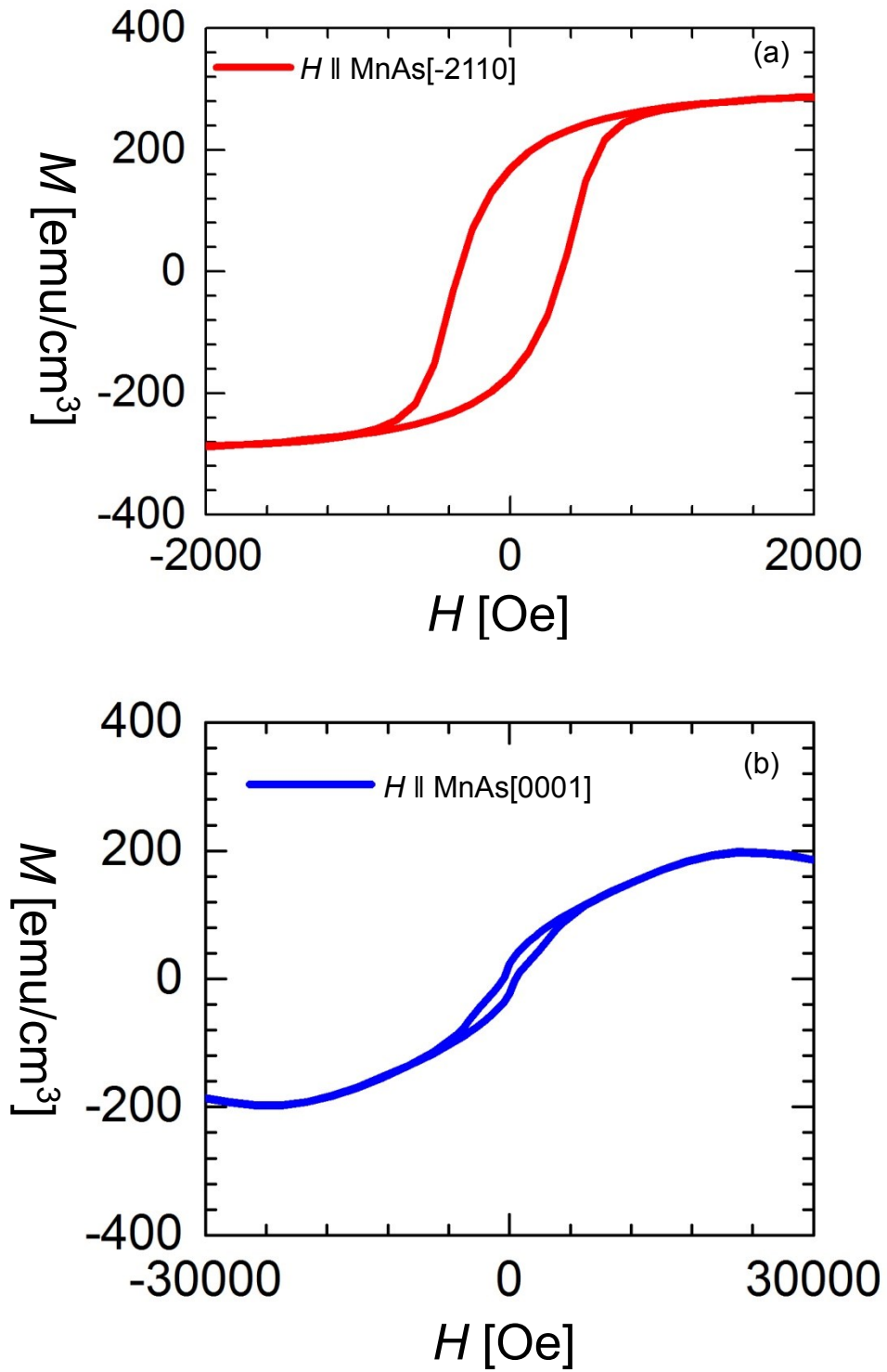
FIG. 5. Magnetization curves along (a) in-plane and (b) out-of-plane directions.

We also studied magnetic phase transition temperature (T_C) of MnAs as a function of temperature at magnetic field of 2000 Oe along [-2110] direction. From Fig. 6(a), we see the sample shows second order phase transition character from ferromagnetic to paramagnetic (FM-PM) transition. In the temperature range between 4 K and 200 K, it seems almost no change of spontaneous magnetization. Above 200 K the sample shows significant decrease of the magnetization with increase of temperature. We also extracted T_C value by first derivative of magnetization versus temperature curve [16] as shown in Fig. 6(b). The minimum gives the T_C ~324 K which is slightly higher than bulk valve of 313 K. The result might originate from some differences between thin film and bulk [17].
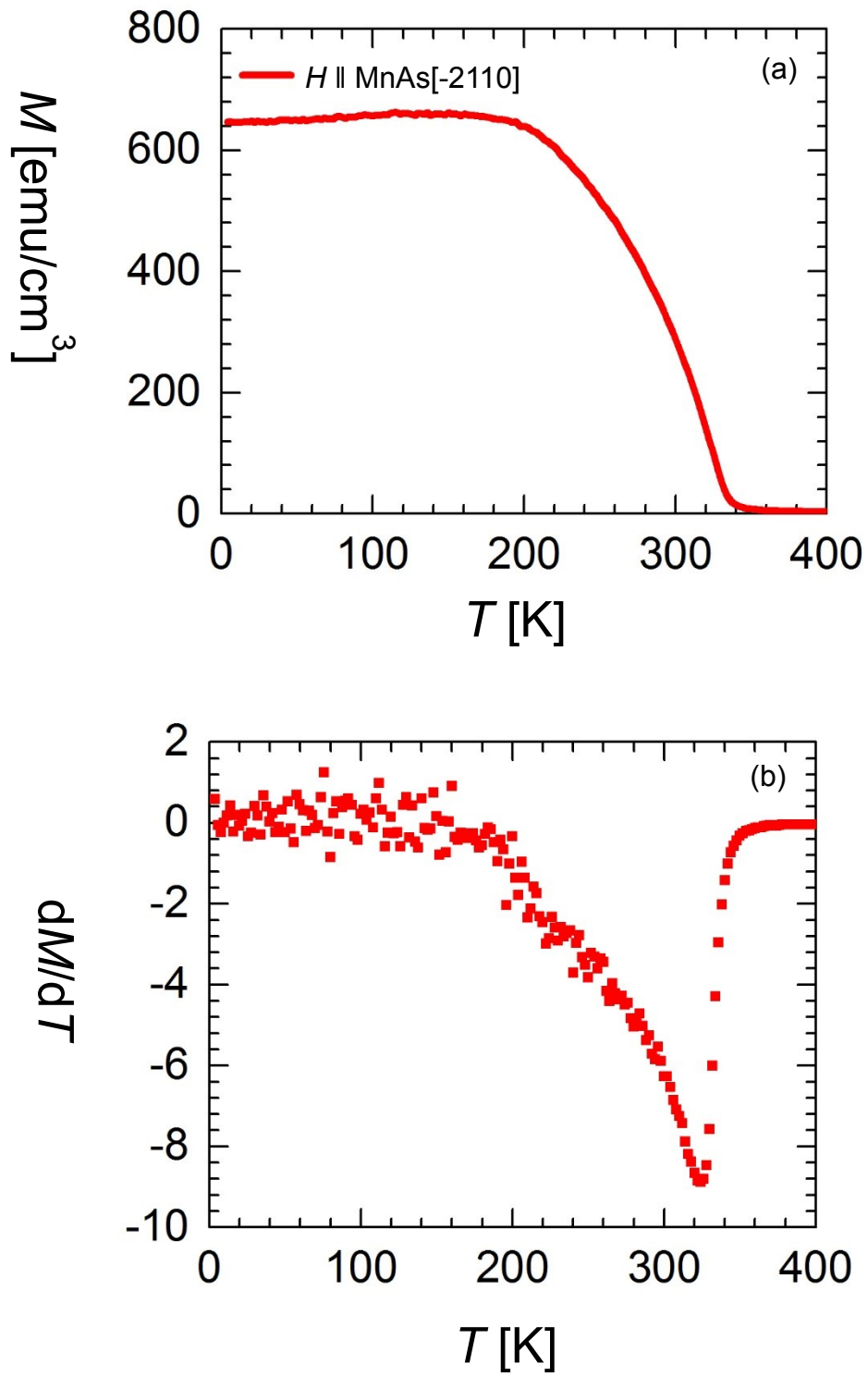
FIG. 6. (a) Magnetization versus temperature curve and (b) its first derivative.

6. Conclusion

We carried out MBE growth of MnAs layer followed by thick InAs layer growth on semi-insulating GaAs(111)B substrate. We confirmed good epitaxial relation of MnAs/InAs to GaAs(111)B by XRD. We also confirmed maze-like magnetic structure with smooth surface by MFM and AFM. We measured magnetization properties of the MnAs/InAs/GaAs(111)B by a SQUID magnetometer, and found easy and hard magnetization along in-plane and out-of-plane directions, respectively, at room temperature. We also confirmed the Curie temperature over room temperature. We believe that the MnAs/InAs hybrid structure on GaAs(111)B can be a base structure for spin-FETs.

Acknowledgement

References

[1] S. Datta and B. Das: Appl. Phys. Lett. 56 (1990) 665.

[2] J. B. Goodenough and J. A. Kafalas: Phys. Rev. 157 (1967) 389.

[3] M. Tanaka, J. P. Harbison, M. C. Park, Y. S. Park, T. Shin, and G. M. Rothberg: Appl. Phys. Lett. 65 (1994) 1964.

[4] E. M. Kneedler, B. T. Jonker, P. M. Thibado, R. J. Wagner, B. V. Shanabrook, and L. J. Whitman: Phys. Rev. B 56 (1997) 8163.

[5] D. Saha, M. Holub, P. Bhattacharya and Y. C. Liao: Appl. Phys. Lett. 89 (2006) 142504.

[6] M. Noguchi, K. Hirakawa, and T. Ikoma: Phys. Rev. Lett. 66 (1991) 2243.

[7] M. Tanaka and K. Takahashi: J. Cryst. Growth 227-228 (2001) 847.

[8] T. W. Kim, H. C. Jeon, T. W. Kang, H. S. Lee, J. Y. Lee, and S. Jin: Appl. Phys. Lett. 88 (2006) 021915.

[9] Y. Morishita, K. Iida, J. Abe, and K. Sato: Jpn. J. Appl. Phys. 36 (1997) L1100.

[10] S. Hara and T. Fukui: Appl. Phys. Lett. 89 (2006) 113111.

[11] L. B. Steren, J. Milano, V. Garcia, M. Marangolo, M. Eddrief, and V. H. Etgens: Phys. Rev. B 74 (2006) 144402.

[12] H. Yamaguchi, J. G. Belk, X. M. Zhang, J. L. Sudijono, M. R. Fahy, T. S. Jones, D. W. Pashley, and B. A. Joyce: Phys. Rev. B 55 (1997) 1337.

[13] I. Vurgaftman, J. R. Meyer, and L. R. Ram-Mohan: J. Appl. Phys. 89 (2001) 5815.

[14] J.E. Ayers: J. Crystal Growth 135 (1994) 71.

[15] Y. Jeong, H. Choi, T. Suzuki: J. Crystal Growth 301-302 (2007) 235.

[16] J. Varalda, A. J. A. de Oliveira, A. Ouerghi, M. Eddrief, M. Marangolo, D. Demaille, V. H. Etgens, N. Mattoso, and D. H. Mosca: J. Appl. Phys. 100, (2006) 093524.

[17] N. Mattoso, M. Eddrief, J. Varalda, A. Ouerghi, D. Demaille, V. H. Etgens, and Y. Garreau: Phys. Rev. B 70 (2004) 115324.